Title

The soil leakage ratio in the Mudu watershed, China

Journal

Environmental Earth Sciences, 75(8)

ISSN

1866-6280

Authors

Wei, Xingping

Yan, Yaner

Xie, Deti

et al.

Publication Date

2016-04-01

DOI

10.1007/s12665-016-5351-9

Peer reviewed

Environ Earth Sci (2016) 75:721
DOI 10.1007/s12665-016-5351-9

ORIGINAL ARTICLE

The soil leakage ratio in the Mudu watershed, China

Xingping Wei[1,2,3] · Yaner Yan[2] · Deti Xie[1] · Jiupai Ni[1] · Hugo A. Loáiciga[3]

Received: 5 May 2015 / Accepted: 7 January 2016 / Published online: 13 April 2016

Abstract Soil leakage in karst areas is an important geomorphic agent of environmental interest. There are several viewpoints concerning soil leakage ratios. One viewpoint states that the soil leakage ratio is high in karst regions, whereas others consider that it is very low. This paper's objective is to describe the soil leakage phenomena qualitatively and quantitatively in the Chongqing Karst, China, by conventional methods such as monitoring runoff plots and paint traces drawn on piles and walls found within runoff plots, and by measuring the activity of the isotope ^{137}Cs at small, medium, and large spatial scales. This paper's results show that soil-filled karst cracks occurred at a small spatial scale with soil leakage ratios ranging from about 3% to about 34% at two abandoned quarries and six soil profiles with rock (karst) crack development. The soil leakage ratio was almost zero at the medium spatial scale. The soil leakage ratio was 4.50% and the surface-soil erosion ratio was 95.50% of the total soil erosion at the large spatial scale. It is concluded that soil leakage ratios in the study area were low at a large spatial scale, and that cracks in karst were filled with soil at small spatial scales. This paper's results indicate that soil leakage phenomena vary depending on the processes acting at the small, medium, and large spatial scales.

Keywords ^{137}Cs · Mudu watershed · Rocky desertification · Runoff plots · Soil leakage · Karst

✉ Yaner Yan
88232075@qq.com

[1] Resources and Environment College, Southwest University, Chongqing 400715, China

[2] Geography and Tourism College, Chongqing Normal University, Chongqing 400047, China

[3] Department of Geography, University of California, Santa Barbara, California 93106, United States

Introduction

Southwest China is known as the largest karst areas in the world, and the regions cover an area of 540,000 km^2 (Yuan et al. 1994; Fan et al. 2011) and occupy approximately 5.2 % of China's territory. Soil erosion can cause rocky desertification, a common type of land degradation in Southwest China that has large impacts on social and economic development. In late 2012, rocky desertification affected about 24 % of the total karst area (Wang et al. 2014). Understanding of surface and underground soil erosion in karst regions is necessary to avoid rocky desertification.

The phenomenon of soil loss in karst areas has been studied from several perspectives including karren, sporopollen, archaeology, and soil nutrients (Jones 1965; Gosden 1968; Bell and Limbrey 1982; Yuan 2009). Radioactive cesium (^{137}Cs) has also been used to observe soil loss. ^{137}Cs is a radioactive nuclide with a half-life of 30.17 year. It was artificially augmented in the environment by nuclear tests during the 1950–1970s, which resulted in a peak fallout rate on the Earth's surface in 1963 (Zapata et al. 2002). ^{137}Cs was rapidly absorbed by topsoil after falling on the ground. ^{137}Cs could resist downward leaching and plant absorption, therefore, subsequent redistribution of ^{137}Cs is associated with the movement of soil particles (Zapata et al. 2002). For this reason, ^{137}Cs is a useful tracer for determining the pathways of soil movement (Hou et al. 2007; Martinez et al. 2010; Bell and Limbrey 1982). A few researchers have documented qualitative descriptions of soil leakage (Zhang et al. 2009; Zhou et al. 2009; Geissen et al. 2007; Kheir et al. 2008), however, quantitative analysis of soil leakage is rare. Soil leakage ratios have also been studied on macroscopic (Vega and Febles 2008; Cao et al. 2008a, b; Xiong et al. 2012; Febles–González et al. 2012) and microscopic scales (Li et al. 2012). Although

several conclusions have been reached, only a few preliminary studies have been conducted on the mechanisms of underground soil leakage in karst areas (She 2009; Wang et al. 2009; Anselmetti et al. 2007).

Two main viewpoints about soil leakage ratios are that they are either high or low in karst areas. Cao et al. (2008a, b) and Xiong et al. (2012) suggested that soil leakage ratios in karst regions of Southwest China are low at a large spatial scale, and only soil filled cracks in the rock were noticed at a small spatial scale. However, Zhang et al. (2007a, b) proposed that soil leakage ratios in the karst region are high. His conclusion was based on the idea that cracks in the rack function as a stone sieve, therefore soil moves deeper into the cracks instead of being lost via surface soil erosion. The debate about soil leakage ratio continues to this date.

Previous soil leakage research in China was mainly carried out in the Guangxi and Guizhou provinces with lesser emphasis given to the Chongqing region. The karst valley topography is predominantly karst terrain in Chongqing, which differs from the terrains in the other provinces. To understand the soil leakage ratio in Chongqing, soil leakage ratios should be studied simultaneously in macroscopic and microscopic spatial scales of karst area. Also qualitatively and quantitatively studies should be conducted at the same time. This approach could provide a reliable basis for understanding soil leakage mechanisms in the karst area. Strongly heterogeneous structure pervades karst areas, while research on underground soil leakage has mainly been concentrated in places such as Guizhou (Li et al. 2006), Yunnan (Wen et al. 2000), Guangxi (Jiang 2014) in China, in the United States (Beynen and Townsend 2005), Italy (Sauro 1993), Spain (Gutiérrez et al. 2008), the Mediterranean regioin (Kheir et al. 2008) and Mexico (Geissen et al. 2007). Nevertheless, there has been limit research undertaken in the karst area of Chongqing. Chongqing is located within the catchment of the Three Gorges Reservoir, and thus soil leakage from this karst area consequently increases sediment deposition in the reservoir. Therefore, studying soil leakage in this region could yield appropriate rationale for government to implement the policies for controlling soil erosion in the Chongqing karst area.

Soil-leakage phenomena in karst is not well understood at present. Currently, there are two dominant opinions about soil leakage. The first one envisions soil moving into underground rivers through karren, rock cracks, and funnel-shaped sinkholes (Zhou et al. 2009; Jiang 2014). The second viewpoints contends that soil moves deeply into cracks and pipelines shaped by karst underground water corrosion or soil moves to the aquifer floor through karren and rock cracks, which do not include for soil into ground river through dolines (Zhang et al. 2007a, b; Geissen et al. 2007; Zhou et al. 2012). The latter viewpoint is adopted in this paper which is depicted in the Fig. 1: soil moves into underground rivers via route *a* and *b*, and this process is termed soil leakage. Alternatively, soil moves into underground rivers via route *c* (Fig. 1) that is not considered as soil leakage.

Materials and methods

Study area

The research was conducted at a site located between north latitudes 28.77° and 39.52°, and between east longitudes 106.45° and 106.90° within the Mudu River Watershed in the Nanping Karst Valley of the Nanchuan District of Chongqing, Southwest China. The area has a typical subtropical monsoon climate, with a mean annual air temperature of 16 °C and an annual average precipitation equal to 1100 mm. Rainfall mainly occurs between June and September. The lithology of the study area is composed of Upper Triassic Xujiahe Formation sandstone (T_3xj), Middle Triassic Leikoupo Formation dolomitic limestone and dolomite (T_2l), Lower Triassic Jialingjiang Formation limestone strata, and Lower Triassic Feixianguan Formation dolomites. The strata feature negligible dipping.

Forty soil-sampling plots, each with an area of 50 × 20 m, were chosen and the average bare rock fraction of the sampling plots was calculated. Nine runoff plots in different land-use types were demarcated and walled-off. The runoff plot locations are shown in Figs. 2 and 3, and the basic data for the runoff plots are listed in Table 1 (Wei 2011). A karst cave named Wangjia Cave was located in the area, and soil from the cave walls was sampled. Six soil profiles with rock cracks were selected near Wangjia Cave and the position of the profiles are shown in Fig. 3. Two abandoned quarries (A and B), which ceased operation in 2008 and 1979, respectively, were selected to count the developed crack rate and soil leakage rate on a local scale. The quarry sites are shown in Figs. 2 and 3.

Field sample collection and methods

Field samples were collected according to the spatial scale (small spatial scale, medium spatial scale and large spatial scale). The small, medium, and large spatial scales focus on the karst crack points, the runoff fields, and the Mudu River watershed, respectively.

Soil leakage at a small spatial scale (abandoned quarries and six soil profiles with karst cracks)

Soil leakage was studied qualitatively by measuring the ^{137}Cs activities at the two abandoned quarries (Fig. 4) and

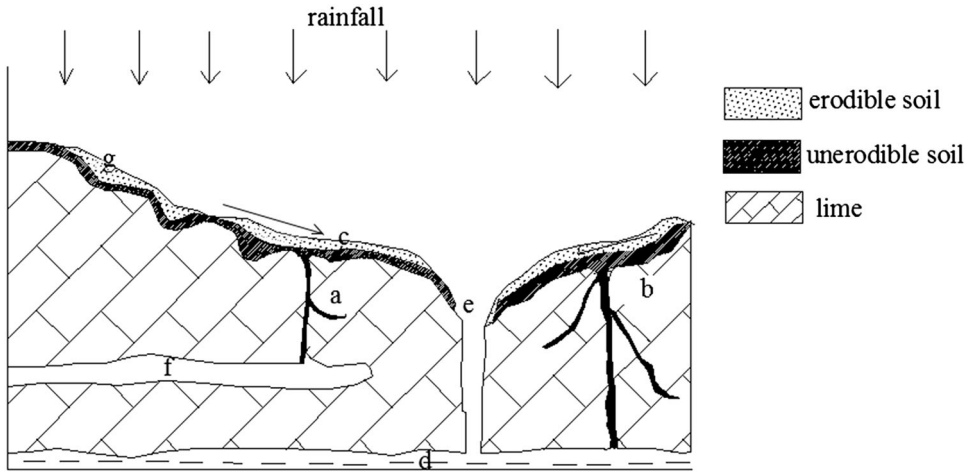

Fig. 1 Concept model of soil leakage (*a* and *b* soil leakage; *g* splash erosion; *c* slope surface erosion; *d* ground river; *e* doline; *f* karst tube erosion)

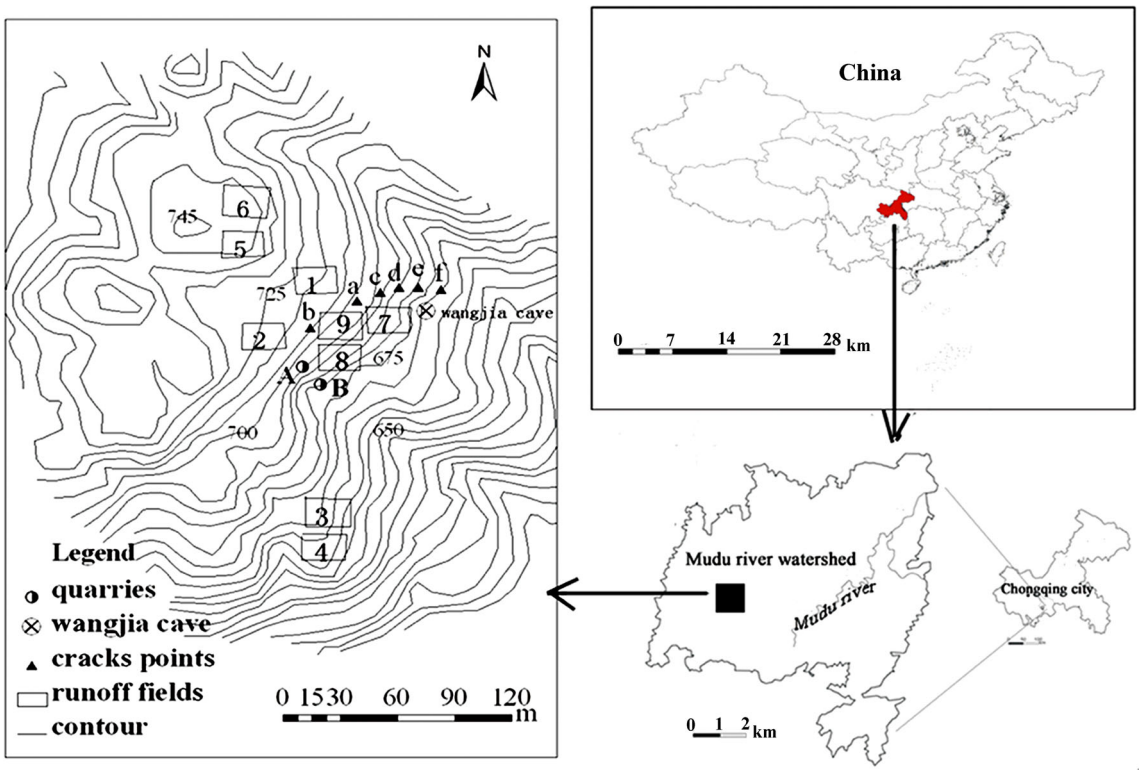

Fig. 2 Location of the research site

six soil profiles with rock cracks. The soil was stratified and sampled at 20 cm depth intervals (or according to the crack developments) to the base rock. The analysis of soil leakage assessed with the measurement of ^{137}Cs activities revealed that in arable layers the ^{137}Cs activity of soil sampled is evenly distributed. The ^{137}Cs activity decreases exponentially with increasing soil depth in non-arable layers. Furthermore, the ^{137}Cs activity was below detection level at soil depths exceeding 40 cm. Evidence of soil leakage would be provided by abrupt increase of the ^{137}Cs activity in soil at depths exceeding 40 cm under the non-arable layer.

The soil leakage ratio was calculated as the area of cracks filled with soil divided by the sum of the areas of cracks filled with soil and of soil overlying the rock. Therefore, the quarry profile was set as a soil reference level, and the soil leakage ratio was calculated as $m/(n + m)$, where m is the profile area of soil filled in cracks and n is the profile area of soil covering the quarry. Similarly, the soil leakage ratio of six soil profiles was calculated.

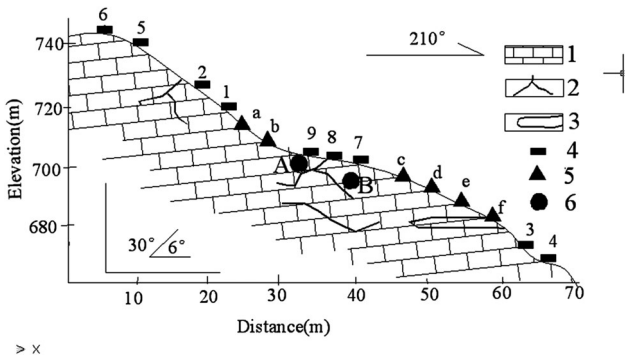

Fig. 3 Profile map of runoff plots position in Nanchuan. *1* limestone of the Jialingjiang group; *2* karst cracks; *3* Wangjia cave; *4* runoff fields; *5* the crack points; *6* abandoned quarries A and B (Letters *a*, *b*, *c*, *d*, *e* and *f* are denoted by a *triangle*, they are the *karst-crack* locations. The numbers *7*, *8* and *9* are denoted by *rectangles*, they are the *runoff* fields)

The reason why soil leakage ratio in small spatial scale is only accounted by soil area are twofold.

Firstly, it is hard to calculate the soil leakage ratio when the soil leakage phenomenon takes place underground. This explains why the majority of methods applied previously to describe the soil leakage phenomenon have been qualitative rather than quantitative. Secondly, these authors selected the rock profile with cracks to study the soil leakage because the cracks developed could be observed. Therefore, the soil leakage ratio could be calculated as the area of cracks filled with soil divided by sum of the areas of cracks filled with soil and of soil overlying the rock. Admittedly, there are limitations to this method. This is because it is impossible or impractical to detect all the cracks filled with soil, thus making the quantification of the area of cracks filled with soil an approximation to its true value. Even with this limitation, however, the calculated soil leakage ratio yields an improved notion over those based purely on qualitative descriptions. This explains why these authors selected the rock profile as a reference profile and use the soil area ratio to calculate the soil leakage ratio. Figure 4 shows a photograph of the abandoned quarries A and B.

Soil leakage on a medium spatial scale (runoff field)

Soil leakage was examined qualitatively by measuring the ^{137}Cs activity changes of soil sampled with the soil depth increasing within the selected runoff fields. The principle is the same as that presented in subsection 2.2.1. The soil in runoff fields 1, 2, 3, 6, and 8 was sampled by selecting four sampling points randomly in each runoff field and sampling a 10 × 10 cm area at 5 cm depth intervals to a depth equal to 40 cm. The soil samples were mixed uniformly for each profile depth and for each runoff field separately and then subjected to ^{137}Cs analysis. The soil leakage was assessed according to the ^{137}Cs concentration changes as a function of soil depth. Figure 5 shows a photograph of the experimental runoff field.

The soil leakage ratio in the runoff plots was determined quantitatively using the conventional methods of drawing paint trace on the wall in runoff plots and drawing paint trace on six wooden piles inserted in the soil at regular intervals in every runoff plots. On December 1, 2008, the conventional method of drawing paint trace on the three walls of each runoff plots and on the wooden piles was

Table 1 Basic parameters of the runoff plots and the sampling point with karst cracks

Number	Landuse types	Latitude/m	Slope (°)	T[(1)](m)	H[(2)](m)	A[(3)](m^2)	R[(4)] (%)
1	Cultivated land	720	12	1.18	0.8	112	40
2	Cultivated land	722	15	1.25	0.8	30	40
3	Cultivated land	675	8	0.35	0.8	50	10
4	Cultivated land	670	10	0.35	0.8	50	15
5	Forest land	742	5	1.20	3.5	120	0
6	Forest land	745	5	1.25	3.5	120	0
7	Honeysuckle land	700	5	0.80	0.5	50	15
8	Honeysuckle land	705	5	1.05	0.5	50	10
9	Grass land	708	5	1.14	0.25	50	12
a	Forest land	715	5	0.40	1.25	80	30
b	Forest land	710	5	0.20	1.34	70	30
c	Wasteland	695	5	1.00	0.50	90	40
d	Wasteland	685	8	0.60	0.45	50	34
e	Wasteland	682	8	0.80	0.49	60	45
f	Wasteland	680	8	0.40	0.50	65	35

(1) *T* soil thickness; (2) Plant community height; (3) Area of land sampled; (4) Bare-rock ratio

Fig. 4 Distribution of cracks and dissolution pores at the abandoned quarries A and B. the quarry profile was regarded as a soil reference level, and the soil leakage ratio was calculated as $m/(n + m)$, where m is the profile area of soil filled in cracks and n is the profile area of soil covering the quarry

implemented at nine experimental runoff fields in the karst area of Nanchuan. The paint trace was drawn where the soil surface intersected the wall and the wooden piles in each runoff plot. This trace defined the height of the surface soil at the measurement locations in each runoff plot. A new paint trace was drawn where the soil surface intersected the walls and the piles at each measurement location after 5 years (on December 12, 2013). The height difference between the old and the new paint traces reflects the depth of soil loss in each runoff field. The total amount of soil erosion included surface soil erosion and soil leakage, which depend on the area and depth of soil loss from a runoff field. The surface soil erosion was the amount of sediment accumulated in the runoff pond. The amount of soil leakage was calculated by subtracting the amount of surface soil erosion from the amount of total soil erosion. The soil leakage ratio was calculated as the ratio of the amount of soil leakage to the total amount of soil erosion.

Soil leakage at a large spatial scale (Mudu River Watershed)

At a large spatial scale, the soil leakage ratio was studied quantitatively using field observations and measurements, followed by sampling and ^{137}Cs measurements. The Mudu River Watershed was regarded as a large spatial scale. The main land-use types in Mudu River watershed included sloped cropland, wood land and grass land, which were determined by a 1:10,000 map of land-use types from the Chongqing Municipal Bureau of Water Resources. Forty random samples with a 10 × 10 cm area and 5 cm depth were chosen on the surface soil in each land-use type. The silt in the ground river was sampled at its entrance into the subsurface and 5 silt samples were collected. The ^{137}Cs activity of silt in the underground river and that of the surface soil from different land-use types over the large spatial scale were measured in the laboratory. The ^{137}Cs activity of surface soil in each land-use type represented the average from 40 soil samples. The ^{137}Cs activity of silt was calculated as the average from 5 silt samples.

The amount of soil erosion associated with different land-use types was estimated by multiplying the area by the modulus of soil erosion for each land-use type. The weight (R) assigned to each land-use type was proportional to the ratio of the amount of soil erosion. The weighted ^{137}Cs activity in the surface soil from the study area was calculated by multiplying the ^{137}Cs activities by the weight assigned to each soil per land-use type. The silt in the underground river involves the ^{137}Cs activities in surface soil and non-soil ^{137}Cs from the interface of soil and rock. The ratio of soil sources was calculated according to the

Fig. 5 *Photograph* of the experimental runoff field and schematic diagram of the experimental runoff field

^{137}Cs activities of silt in the underground river, that of the surface soil, and that of the underground soil. The ratio method (Wen et al. 2000) summarized by Equs. 1 through 4 was used to calculate amounts of soil erosion in land-use types a, b, and c, which represent slope cropland, wood land, and grass land, respectively.

$$Q_a = S_a \times M_a, \quad Q_b = S_b \times M_b \quad \text{and} \quad Q_c = S_c \times M_c \tag{1}$$

$$C_1 = C_a \times R_a + C_b \times R_b + C_c \times R_c \tag{2}$$

$$f_m + f_n = 100\ \% \tag{3}$$

$$C_2 = C_1 \times f_m \tag{4}$$

C_1 denotes the ^{137}Cs activity of the surface soil (Bq kg^{-1}); C_a, C_b, and C_c represent the ^{137}Cs activity of slope cropland, wood land, and grass land respectively; R_a, R_b, and R_c are the weights of soil erosion in slope cropland, wood land, and grass land respectively; Q_a, Q_b, and Q_c denote the amounts of soil erosion in slope cropland, wood land, and grass land respectively (t/year); M_a, M_b, and M_c are the soil erosion modules (t/(km^2 year)) in slope cropland, wood land, and grass land respectively; S_a, S_b, and S_c are the areas (km^2) of slope cropland, wood land, and grass land respectively; C_2 denotes the^{137}Cs concentration of ground river silt (Bq·kg^{-1}); f_m is the surface soil erosion ratio, and f_n is the soil leakage ratio.

Measurement of ^{137}Cs concentration

Soil samples were tested after they were air-dried, grilled, sieved through 2 mm mesh, and weighed. Soil samples taken from small, medium, and large spatial scales were sent to the isotopic laboratory at the Institute of Mountain Hazards and Environment, Chinese Academy of Science for ^{137}Cs concentration analysis. The ^{137}Cs concentration was calculated according to the 662 keV spectrum peak area, and analytical errors were kept within ±5 % (95 % confidence limits). The samples weighed ≥250 g and the testing time was ≥33,000 s.

Results

Soil leakage and soil leakage ratio at a small spatial scale

Soil leakage determined qualitatively by ^{137}Cs activity of soil sampled at both the two abandoned quarries and six soil profiles with karst cracks

Soil leakage situation was determined qualitatively by the ^{137}Cs activity. Soil filled racks at the abandoned quarries and at the six soil profiles were sampled, and the ^{137}Cs activities of the soil samples were measured (Table 2). Although the ^{137}Cs activity in profiles A, B, *a*, *b*, and *f* decreased exponentially with increasing soil depth, small ^{137}Cs activities were detected beneath 40 cm soil layer. Small soil leakage takes place in such profiles. No regular pattern was discerned in profiles *c*, *d*, and *e* where ^{137}Cs activity can be detected even at 60, 90 and 100 cm soil depths. Larger soil leakage takes place in profiles *c*, *d*, and *e*. The ^{137}Cs activity was undetectable at certain soil depth from the surface in all profiles, which illustrates the soil leakage depth is limited. At the same time, soil from the walls of the Wangjia Cave was collected for measuring its ^{137}Cs activity. No ^{137}Cs activity was detected, which indicates that the surface soil did not leak into the cave through the karst cracks.

Table 2 ^{137}Cs changes in soil profile with depth

Sampling point	Depth of the sample (cm)	^{137}Cs concentration (mBq/g)	Sampling point	Depth of the sample (cm)	^{137}Cs concentration (mBq/g)
a	0	15.7	f	0	1.04
	20	0		20	0
	40	0.76		40	0.65
	60	0.42		60	0
	80	Non-fractured rock		80	0.74
	100			91	0.31
	120			140	0
	160			160	0
b	0	22.71	c	0	9.92
	20	0.52		20	2.55
	40	0.03		40	0
	60	Non-fractured rock		60	0
	80			80	0.33
	100			100	1.09
	120			150	0.18
	140			200	0
	160			250	0
d	0	4.6	e	0	1.65
	20	1.3		20	1.21
	60	1.12		40	0
	90	1.03		60	1.32
	115	0.42		90	0
	150	0.46		120	0.83
	175	0.76		175	0.76
A	0	4.75	B	0	5.42
	20	2.01		20	1.47
	45	1.02		40	0.82
	70	0.45		60	0.56
	90	0.68		90	0.31
	100	0.05		110	0.12
	150	0		150	0
	200	0		190	0.04
	250	0		300	0

Soil leakage ratio calculated as the ratio of soil-filled karst-crack area to overlying soil area at the two quarries

The area ratio of soil-filled cracks was about 5 % in profile A and 3 % in profile B indicating a greater development of cracks in profile A than in profile B. There were more cracks at higher elevations than at lower elevations in both profiles. And the area ratio at six soil profiles with the rock cracks *a–f* is about 13, 14, 18, 34, 23 and 15 % successively. The soil leakage ratio indicated the development of the rock cracks at the abandoned quarries is lower than that of the six soil profiles.

Soil leakage and soil leakage ratio at a medium spatial scale

Soil leakage determined qualitatively using ^{137}Cs activity

To study the conditions of soil leakage, the soil in the runoff plots was sampled at 5 cm intervals. If soil leakage existed, then ^{137}Cs activities should increase with soil depth. The ^{137}Cs activities at runoff plots 1, 2, 3, and 6 were close to zero beneath a soil depth of 30 cm. The ^{137}Cs activities at runoff plot 8 were much higher even at a depth of 40 cm than those in other plots. To verify whether soil

Table 3 ^{137}Cs concentration (mBq/g) distribution of various land-use types at the runoff field in Nanchuan

Soil depth (cm)	J1	J2	J3	J6	J8
0–5	1.23	1.33	1.66	7.33	6.67
5–10	1.03	1.23	1.51	6.54	5.71
10–15	1.03	1.32	1.29	6.78	6.35
15–20	0.52	0.56	1.1	7.35	9.08
20–25	0.34	0.37	0	7.15	8.35
25–30	0	0.05	0	5.59	9.83
30–35	0	0	0.43	0.91	8.1
35–40	0	0	0.42	0.24	11.02
40–45					10.45
45–50					8.34
50–55					6.23
55–60					5.35
60–65					0.23
65–70					0
70–80					0
80–90					0
90–100					0

J1, J2, J3, J6, and J8 denote runoff field number 1, 2, 3, 6 and 8, respectively

leakage existed at runoff plot 8, the soil at the depth between 40 and 100 cm was resampled. The ^{137}Cs activities at runoff plot 8 was zero beyond the depth of 65 cm. The reason that ^{137}Cs activity reached up to the depth of 65 cm is that the elevation of runoff plot 8 is relatively low so soil from other areas could also be accumulated there. Therefore, it is reasonably conclude that soil leakage does not exist at runoff plot 8 (Table 3).

All 3 runoff plots were croplands. Among them, plots 1 and 2 are natural slopes, while plot 3 is an altered slope with soil transference and accompanies with fertilizer applications as well. Fertilized soil was resistant to soil erosion, as a result, ^{137}Cs activity in the surface soil of runoff plot 3 was larger than those of plot 1 and 2. The soil erosion intensities were similar between runoff plots 1 and 2. According to the ^{137}Cs distribution in the profile, ^{137}Cs activities were evenly distributed within the plow layer, but declined exponentially beneath this layer, indicating that there was no soil leakage at runoff plots 1, 2, or 3. Runoff plot 6 was forested land, and the ^{137}Cs activity of the surface soil was higher than that in the sloped cropland and was detected down to 30 cm depth from the surface. This phenomenon could be explained by weak surface soil erosion at runoff plot 6. Runoff plot 8 is honeysuckle land, and ^{137}Cs was detected in the area reached to 40 cm depth from the surface. This might due to lower altitude and soil accumulation from higher altitude areas. The distribution of ^{137}Cs in runoff plot 8 indicates that soil leakage did not take place there.

Soil leakage ratio determined quantitatively by the drawing paint trace method in runoff plots

Soil leakage ratios in the nine runoff plots were monitored by drawing paint traces on the walls in each runoff plots for five consecutive years. The average soil leakage ratio in the nine runoff plots was zero during the 5 years (Table 4). The following reasons could explain the absence of soil leakage in the runoff plots area. First, limited research funds led to the selection of runoff plots without high bare rocks. Second, there was no karst crack development in the bedrock of the chosen runoff plots.

Soil leakage ratio based on Mudu River at a large spatial scale

The proportion of surface soil erosion to ground soil erosion was calculated for the Mudu River Watershed. The areas included woodland (487,580 hm^2), sloped cropland (832,197 hm^2), and grassland (142,101 hm^2) according to

Table 4 Average proportions of the surface and underground erosion at the runoff field in Nanchuan (standard deviation within parentheses)

The number of the runoff field	The total amount of soil erosion (t/km^2 a)	Surficial soil loss amount (t/km^2 a)	Soil leakage amount (t/km^2 a)	The ratio of soil leakage (%)
J1	40.5 (4.56)	40.5 (4.56)	0	0
J2	33.82 (4.91)	33.82 (4.91)	0	0
J3	22.99 (4.64)	22.99 (4.64)	0	0
J4	27.92 (4.64)	27.92 (4.64)	0	0
J5	7.74 (1.03)	7.74 (1.03)	0	0
J6	9.43 (1.56)	9.43 (1.56)	0	0
J7	14.24 (1.39)	14.24 (1.39)	0	0
J8	11.75 (0.56)	11.75 (0.56)	0	0
J9	9.31 (1.49)	9.31 (1.49)	0	0

Table 5 ^{137}Cs concentration and allocation ratio between the arable land, forest land, the grassland and silt of the ground river at the runoff field in Nanchuan

	^{137}Cs quality activity (mBq/g)	Weighted value[a]
Sloped cropland	1.41	0.71
Wood land	7.33	0.26
Grass land	6.67	0.03
The silt of ground river	2.97	

[a] Weighted value in different land-use types is proportional to the amount of soil erosion in different land-use types

the 1:10,000 map of land-use types from field surveys. The amount of soil erosion in woodland, sloped cropland, and grassland was 25, 40, and 10 t km^2 yr^1, respectively, based on runoff plot monitoring. According to the area and erosion modulus, the amount of soil eroded each year from woodland, grassland, and sloped cropland was 12,189,500, 33,287,880, and 1,421,010 t; respectively. Accordingly, the weights of eroded soil for the three land-use types were 0.26, 0.71, and 0.03 (Table 5).

With the combination of ^{137}Cs activities of the three land-use types and the weight, the mean ^{137}Cs activity in the surface soil was about 3.11 mBq/g ($1.41 \times 0.71 + 7.33 \times 0.26 + 6.67 \times 0.03 = 3.11$). The silt in the underground river came from two sources: the soil at the boundaries between rock and soil, and the surface soil through sinkholes, shafts and other conduits into the underground river. The soil at the rock–soil interface did not contain measurable ^{137}Cs, while, the ^{137}Cs activity in the soil from the surface to the underground river was about 3.11 mBq/g, and the ^{137}Cs activity in the silt from the underground river equaled 2.97 mBq/g (Table 5). Therefore, the proportion of soil lost from the surface and underground erosion was 95.50 and 4.50 %, respectively, according to the ^{137}Cs activity and the ratio method.

Discussion

The results herein reported for the soil leakage ratios may be due to the following reasons. First, few previous studies of underground soil leakage have been conducted simultaneously at macroscopic scales and microscopic scales of analysis. Second, most underground soil leakage studies have been qualitative in nature, which hinders our understanding of soil erosion mechanisms in karst areas.

The soil leakage ratio in Chongqing karst was studied simultaneously in macroscopic and microscopic spatial scales of karst area. Also qualitatively and quantitatively studies must be carried out simultaneously. This study concludes that the soil leakage ratios were low in the study area. The soil leakage ratios were in the range from 3 to 34 % at the small spatial scale, zero at the medium spatial scale, and about 4.5 % at the large spatial scale. These results are different from those of other karst areas which have a high soil leakage ratio (Wang et al. 2014; Luo et al. 2008; Zhang et al. 2007a, b). The reasons are as follows: Firstly, karst landform leads to the low soil leakage ratio in study area. Karst valley landform predominates in Chongqing while peak cluster depression, hoodoos and so on landforms are the main karst landform in Guangxi, Guizhou and Yunnan provinces of Southwest China. The difference of karst landform cause varying dynamic interactions between the surface karst zone and groundwater. The dynamic link is weak in Chongqing while it is very strong in Guangxi, Guizhou and Yunnan provinces. Therefore, soil leakage phenomena is limited by the weak dynamic interaction existing in Chongqing, whereas the soil leakage phenomenon is more prevalent under strong dynamic interactions found in Guangxi, Guizhou, and Yunnan province. Secondly, soil fills cracks through soil leakage at small, medium, and large spatial scales. Therefore, it is very difficult for soil to move downward into underground rivers through these cracks. Moreover, the moss and plant roots adhere to the soil filled in the crack, which prevents the downward transport of soil. In addition, soil overlying a crack can sometimes form an arch that prevents the soil from falling into the crack. With further dissolution of carbonate rocks, more soil can combine to form a more stable soil arch. Last but not the least, crack development is slow in the study area, therefore there is no space for the surface soil to be transported deeper, which restricted the soil leakage in our study area. However, soil leakage could occur Only when external forces such as construction, mining and agricultural activities affect the stability of a soil arch, and causes their collapse to form a sinkhole, which are common in karst regions(Zhou and Beck 2008). This is why soil leakage occurs in areas with high-impact human activities such as farming. Similarly, soil erosion from cultivated areas is typically higher than uncultivated areas (Theocharopoulos et al. 2003).

In this paper's study area, surface soil was transported into underground rivers mainly through sinkholes, vertical shafts, and funnels with a low soil leakage ratio. The high heterogeneity of geological structures in this study's karst region causes the difference in crack development that

explains its lower soil leakage ratio compared to those of other karst regions.

Conclusion

Soil leakage takes place at a small spatial scale, while soil leakage phenomenon is variable according to the soil leakage ratio at medium spatial scales. Soil leakage ratios at a large spatial scale in the study area are low. In this paper's study region surface soil erosion predominates over underground soil erosion. Soil-filled cracks in rocks is immobilized because it adheres to moss and tree roots in the cracks. Although soil leakage and surface soil erosion and low pedogenic rates are the causes of rocky desertification, we believe that population pressures and the low soil formation rates are the major reasons for rocky desertification in our study areas.

Further studies of the mechanisms of soil leakage are essential for understanding the differences in soil leakage ratios observed in our study area those reported elsewhere. New and more reliable methods for monitoring soil leakage phenomena would lead to improved results in this field of inquiry. This paper's results represent a first step in the quest for quantitative characterization of soil leakage ratios in the Chongqing karst region. Other study areas must be pursued to obtain further data and refinement of our findings in Chongqing.

Acknowledgments The author would like to thank the reviewers for their insightful comments and helpful suggestions on submitted manuscript. This research was financially supported by the National Natural Science Foundation of China (Grant No. 41202135) and the Natural Science Foundation of Chongqing, China (Grant No. cstc2012jjA80008). The authors also thank the financial award from State Scholarship Fund of China Scholarship Council (File No. 201504500006) to support the research at UCSB.

References

Anselmetti FS, Hodell DA, Ariztegui D, Brenner M, Rosenmeier MF (2007) Quantification of soil erosion rates related to ancient Maya deforestation. Geol 35:915–918

Bell M, Limbrey S (1982) Archaeological aspects of woodland ecology. BAR Int Series 29:115–127

Beynen PV, Townsend K (2005) A disturbance index for karst environments. Environ Manage 36(1):101–116. doi:10.1007/s00267-004-0265-9

Cao JH, Jiang ZC, Yang DS, Pei JG, Yang H, Luo WQ (2008a) Soil loss tolerance and prevention and measurement of karst area in southwest China. Soil Water Conserv China 12:40–45 **(in Chinese)**

Cao JH, Jiang ZC, Yang DS, Pei JG, Yang H, Luo WQ (2008b) Grading of soil erosion intensity in Southwest karst area of China. Sci Soil Water Conserv 6:1–7 **(in Chinese)**

Fan FD, Wang KL, Xiong Y, Xuan Y, Zhang W, Yue YM (2011) Assessment and spatial distribution of water and soil loss in karst regions, southwest China. Acta Ecologica Sinica 31(21): 6353–6362 **(in Chinese)**

Febles-González JM, Vega-Carreño MB, Amaral-sobrinho NMB, Tolõn-becerra A, Lastra-bravo XB (2012) Soil loss from erosion in the next 50 years in karst regions of mayabeque province, Cuba. Land Degrad Develop 25:573–580. doi:10.1002/ldr.2184

Geissen V, Kampichler C, López-de Llergo-Juárez JJ (2007) Superficial and subterranean soil erosion in Tabasco, tropical Mexico: development of a decision tree modeling approach. Geoderma 139:277–287

Gosden MS (1968) Peat deposits of Scar Close Ingleborough, Yorkshire. J Ecol 56:345–353

Gutiérrez F, Cooper AH, Johnson KS (2008) Identification, prediction and mitigation of sinkhole hazards in evaporate karst areas. Environ Geol 53:1007–1022. doi:10.1007/S00254-007-0725-4

Hou JC, Li ZB, Li M (2007) Preliminary study on spatial distribution of soil erosion in a small watershed in purple hilly area using 137Cs tracer. Trans CSAE 23(3):46–50 **(in chinese)**

Jiang ZC (2014) The leakage of water and soil in the karst Peak cluster depression and its prevention and treatment. Acta Geosci Sinica 5:535–542 **(in Chinese)**

Jones RI (1965) Aspects of the biological weathering of limestone pavements. Proc Geol' Assoc 76:421–434

Kheir RB, Abdallah C, Khawlie M (2008) Assessing soil erosion in Mediterranean karst landscapes of Lebanon using remote sensing and GIS. Eng Geol 99:239–254

Li YB, Wang SJ, Wei CF, Long J (2006) The spatial distribution of soil loss tolerance in carbonate area in Guizhou province. Earth Environ 34:36–40 **(in Chinese)**

Li J, Xiong KN, Wang XP (2012) Observation of subterranean soil and water loss of karst area. Soil Water Conserv China 6:38–40

Luo WQ, Jiang ZC, Han QT, Cao JH, Pei JG (2008) Soil distribution and soil erosion characteristics in different geomorphological positions in peak cluster and depression. Soil Water Conserv China 12:46–49 **(in Chinese)**

Martinez C, Hancock GR, Kalma JD (2010) Relationships between 137Cs and soil organic carbon (SOC) in cultivated and never-cultivated soils: an Australian example. Geoderma 4(19):35–45

Sauro U (1993) Human impact on the karst of the Venetian ForeAlps, Italy. Environ Geol 21:115–121

She TY (2009) The study on soil leakage mechanism in karst region in Guizhou. The Institute of Civil Engineering in Tongji University, Guiyang, p 28 **(in Chinese)**

Theocharopoulos SP, Florou H, Walling DE (2003) Soil erosion and deposition rates in a cultivated catchment area in central Greece, estimated using the 137Cs technique. Soil Tillage Res 69:153–162

Vega MB, Febles JM (2008) Application of the new method of evaluation of the soil erosion (EVERC) and the model MMF in soils of the Mamposton cattle production basin in Havana province Cuba. Cuban J Agric Sci 42:299–304

Wang HS, Xiong KN, Liu Y (2009) Mechanism research of soil and water loss underground in karst region. Soil Water Conserv China 8:11–15 **(in Chinese)**

Wang JX, Zou BP, Liu Y, Tang YQ, Zhang XB, Yang P (2014) Erosion-creep-collapse mechanism of underground soil loss for the karst rocky desertification in Chenqi village, Puding county, Guizhou, China. Environ Earth 72:2751–2764. doi:10.1007/s12665-014-3182-0

Wei XP (2011) The study on the characteristics and mechanism of soil erosion in karst valley area, Chongqing. Southwest University, Chongqing, p 16 **(in Chinese)**

Wen AB, Zhang XB, Wang YK, Wang JW, Huo TR, Zhang YY, Xu JY, Bai LX (2000) Study on sedimentation source using caesium-137 Technique in Yungui plateau region of upper Yangtze river. J Soil Water Conserv 14(2):25–28 **(in Chinese)**

Xiong KN, Li J, Long MZ (2012) Features of soil and water loss and key issues in demonstration areas for combating karst rocky desertification. Acta Geographica Sinica 67:878–888 **(in Chinese)**

Yuan H (2009) Study on soil capability of nutrient's holding and soil degradation in karst area. Southwest University, Chongqing, pp 99–101 **(in Chinese)**

Yuan DX, Zhu DH, Weng JT (1994) Karstology in China. Geological Publishing House, Beijing **(in Chinese)**

Zapata F, Garcia-Agudo E, Ritchie JC, Appleby PG (2002) Introduction. In: Zapata F (ed) Handbook for the assessment of soil erosion and sedimentation using environmental radionuclides. Kluwer, Dordrecht, pp 1–13

Zhang XB, Jiao JY, He XB, Wen AB, He YB, Zhang YQ, Long Y (2007a) Soil loss tolerance and reasonable soil loss. Sci Soil Water Conserv 5:114–116 **(in Chinese)**

Zhang XB, Wang SJ, He XB, Wang YC, He YB (2007b) Soil creeping in weathering crusts of carbonate rocks and underground soil losses on karst slopes. Earth Environ 35:202–206 **(in Chinese)**

Zhang XN, Wang KL, Zhang W, Chen HS, He XY, Zhang XB (2009) Distribution of ^{137}Cs and relative influencing factors on typical karst sloping land. Environ Sci 30:3152–3158 **(in Chinese)**

Zhou WF, Beck BF (2008) Management and mitigation of sinkholes on karst lands: an overview of practical applications. Environ Geol 55:837–851. doi:10.1007/s00254-007-1035-9

Zhou NQ, Li CX, Jiang SM, Tang YQ (2009) Models of soil and water loss and soil leakage in puding karst area. Bull Soil Water Conserv 29:7–11 **(in Chinese)**

Zhou J, Tang YQ, Yang P, Zhang XH (2012) Inference of creep mechanism in underground soil loss of karst conduits I. Conceptual model. Nat Hazards 62:1191–1215. doi:10.1007/s11069-012-0143-3